COMMUNICATIONS IN NUMERICAL METHODS IN ENGINEERING
Commun. Numer. Meth. Engng 2003; **19**:847–863 (DOI: 10.1002/cnm.635)

A linearized implicit pseudo-spectral method for some model equations: the regularized long wave equations

K. Djidjeli[1], W. G. Price[1], E. H. Twizell[2,*] and Q. Cao[3]

[1]*School of Engineering Sciences, Ship Science, University of Southampton, Southampton SO17 1BJ, U.K.*
[2]*Department of Mathematical Sciences, Brunel University, Uxbridge, Middlesex UB8 3PH, U.K.*
[3]*Department of Engineering, University of Liverpool, Liverpool L69 3GH, U.K.*

SUMMARY

An efficient numerical method is developed for the numerical solution of non-linear wave equations typified by the regularized long wave equation (RLW) and its generalization (GRLW). The method developed uses a pseudo-spectral (Fourier transform) treatment of the space dependence together with a linearized implicit scheme in time.

An important advantage to be gained from the use of this method, is the ability to vary the mesh length, thereby reducing the computational time. Using a linearized stability analysis, it is shown that the proposed method is unconditionally stable. The method is second order in time and all-order in space.

The method presented here is for the RLW equation and its generalized form, but it can be implemented to a broad class of non-linear long wave equations (Equation (2)), with obvious changes in the various formulae.

Test problems, including the simulation of a single soliton and interaction of solitary waves, are used to validate the method, which is found to be accurate and efficient. The three invariants of the motion are evaluated to determine the conservation properties of the algorithm. Copyright © 2003 John Wiley & Sons, Ltd.

KEY WORDS: regularized long waves (RLW); solitary and periodic wave solutions; homoclinic and periodic orbits; pseudo-spectral; linearized implicit method; unconditional stability

1. INTRODUCTION

A fundamental problem of interest in fluid mechanics is to provide an accurate description of the waves on a water surface. Shortly after the experiments of Russell [1], Stokes [2] developed approximate expressions for non-linear periodic waves in deep water and Boussinesq [3] and Rayleigh [4] obtained approximate expressions for the solitary wave. By the end of the 19th century, an adequate theory for solitary waves had been developed, in the form of a modified wave equation known as the Korteweg–de Vries, or KdV equation [5]. Derived from basic equations of fluid dynamics, the KdV equation describes how

*Correspondence to: E. H. Twizell, Department of Mathematical Sciences, Brunel University, Uxbridge, Middlesex UB8 3PH, U.K.

Received 22 July 2002
Accepted 13 February 2003

waves propagate under the influence of gravity in one direction in shallow water. The regularized long wave (RLW) equation [6, 7] has been proposed as an alternative (and, in some, respect, more suitable—better-posed) model governing the evolution of long waves in non-linear dispersive systems to the more usual KdV equation. It has been shown to have solitary wave solutions and to govern a large number of important physical phenomena such as shallow water waves and plasma waves [6, 8, 9]. However, unlike the KdV equation, the RLW equation is not completely integrable. Numerical investigations [9–12] have confirmed that solitary-wave interactions are inelastic, while theoretical studies reveal only three conservation laws [13].

Few analytic solutions are known. Moreover, there are many examples of inexact, quasi-soliton or n_s-solitary wave behaviour ($n_s \geqslant 2$) where little or no analytical results are known and thus numerical studies using accurate numerical methods are essential in order to develop an understanding of the phenomena. The numerical solution of the RLW equation has been the subject of many papers. Various numerical studies have been reported based on the finite difference [6, 14–16], splitting [16, 17], Galerkin [18, 19], finite element (based on quadratic/cubic B-spline and the least-square finite elements) [11, 12, 20–23], and pseudo-spectral methods [10]. A recent comparative study in Reference [24] has shown that the linearized implicit pseudo-spectral scheme provides a high accurate and efficient method for solitary wave solutions of the KdV equation and its generalized form. Fornberg and Whitham's pseudo-spectral method [25] for the solution of the KdV equation, and Sloan's pseudo-spectral method [10] for the RLW equation are found to be efficient for physical problems with periodic boundary conditions. They are second-order accurate in time and all order in space. However, these methods are only conditionally stable. For example, for the KdV equation, the linearized stability condition of the pseudo-spectral method is $\Delta t/\Delta x^3 < 3/2\pi^2 \simeq 0.1520$ [25], while for the RLW equation, the condition for the stability of the Sloan method [10] is $\Delta t < 2\sqrt{\mu}/\beta$ (i.e. small Δt is needed if μ is small or β large). These restrictions may render these methods unsuitable for use with some problems. To overcome this difficulty, the linearized implicit pseudo-spectral method (which uses a Fourier transform treatment of the space dependence together with a linearized implicit scheme in time) developed in Reference [24] will be extended to the RLW equation and its generalized form. Using the linearized stability analysis, it is shown that the proposed method is unconditionally stable.

2. GOVERNING EQUATIONS

In the study of non-linear waves, a number of basic equations take the form

$$u_t + u_x + f(u)u_x + Lu = 0, \quad t > t_0, \ -\infty < x < \infty \tag{1}$$

where $f(u)$ is a function of u and L is a linear operator with constant coefficients. For $f(u) = u$, and $Lu = \mu u_{xxx}$ (or $Lu = -\mu u_{xxxxx}$), Equation (1) reduces to the third- and fifth-order KdV equation, respectively. An efficient numerical scheme based on the linearized implicit pseudo-spectral method was developed for solving the third- and fifth-order KdV equations (and their generalized forms) [24].

Among the model equations proposed as alternatives to the non-linear wave equation (1) is

$$u_t + u_x + f(u)u_x + (Hu)_t = 0, \quad t > t_0, \ -\infty < x < \infty \tag{2}$$

where the linear operator H belongs to a class of pseudo-differential operators [7]. In the present work, we shall be particularly interested in the RLW equation given by

$$u_t + u_x + uu_x - \mu u_{xxt} = 0 \tag{3}$$

and its generalized form [26]

$$u_t + u_x + u^m u_x - \mu u_{xxt} = 0 \tag{4}$$

where μ models the dispersion.

The linearized implicit pseudo-spectral method developed in Reference [24] will be extended to the RLW equation and its generalized form. The numerical scheme is developed for a periodic initial-value problem in which u is a given function at $t = t_0$ and the solution is periodic in x outside the interval $a < x < b$. For most of the problems considered, a and b may be chosen large enough so that the boundaries do not affect the wave interactions.

The method developed here will be described in terms of Equations (3) and (4), but it can be implemented to a broad class of equations of form (2), with obvious changes in the various formulae. A brief description on how this method can be extended to solve Equation (2) is outlined at the end of Section 3.

2.1. Solitary and periodic wave solutions

The RLW equation (3) and its generalized form (4) admit soliton type solutions [27, 28]. Travelling wave solutions of (4) are of the form $u = \varphi(X)$ with $X = x - (1 + c)t$, where c is the wave speed. Replacing $u = \varphi(X)$ in Equation (4), leads to an ordinary differential equation given by

$$-c\varphi' + \varphi^m \varphi' + \mu(1 + c)\varphi''' = 0 \tag{5}$$

where $\varphi' = \mathrm{d}\varphi(X)/\mathrm{d}X$. Integrating equation (5) leads to

$$-\frac{c}{\mu(1 + c)}\varphi + \frac{1}{\mu(1 + c)(m + 1)}\varphi^{m+1} + \varphi'' = 0 \tag{6}$$

For $m = 1$ and 2, Equation (6) reduces to the Helmholtz oscillator and Duffing equations, respectively. These equations are found to play an important role in the understanding of some physical problems, for example, the capsizing of ships in waves, forced vibrations of a cantilever beam in the non-uniform field of two permanent magnets (see, for instance, References [29–32]). These equations are found to have periodic and chaotic solutions.

Letting $u = \varphi$ and $u' = v$ in Equation (6), it follows that

$$u' = v \quad \text{and} \quad v' = \frac{c}{\mu(1 + c)}u - \frac{1}{\mu(1 + c)(m + 1)}u^{m+1} \tag{7}$$

The Hamiltonian of the system of Equations (7) is given by

$$H(u, v) = \frac{1}{2}v^2 - \frac{1}{2}\frac{c}{\mu(1 + c)}u^2 + \frac{1}{\mu(1 + c)(m + 1)(m + 2)}u^{m+2} \tag{8}$$

Definition
A system is said to satisfy **condition A**, if $m = p/q$, where p is even (q and p are relatively prime integers), otherwise the system is said to satisfy **condition B**.

Theorem
For the system of Equations (7), $(0,0)$ is a saddle point. If condition A is satisfied, the saddle point $(0,0)$ is connected by two homoclinic orbits in each of which there is a centre point given by $(u_{\pm}, v) = (\pm(c(m+1))^{1/m}, 0)$, otherwise, if condition B is satisfied, the saddle point $(0,0)$ is connected by one homoclinic orbit in which there is a centre point, given by $(u, v) = ((c(m+1))^{1/m}, 0)$.

As the dynamical behaviour in the system with condition B can occur in the system with condition A, it is sufficient, here, to consider Equation (6) with condition A only.

The level set of $H(u,v) = 0$ consists of one saddle point (0,0) and two homoclinic orbits Γ_+ and Γ_- passing through $q_{\pm}(0) = (\pm(c(m+1)(m+2))^{1/m}, 0)$. It can be shown that the trajectories Γ_+ and Γ_- are given by

$$\begin{aligned} q_+(X) &= \left(A_0 \operatorname{sech}^{2/m}(B_0 X), -\frac{2}{m} A_0 B_0 \operatorname{sech}^{2/m}(B_0 X) \tanh(B_0 X)\right) \\ q_-(X) &= -q_+(X) \end{aligned} \tag{9}$$

where

$$A_0 = \left(\frac{c}{2}(m+1)(m+2)\right)^{1/m} \quad \text{and} \quad B_0 = \frac{m}{2}\sqrt{\frac{c}{1+c}}$$

The solution $A_0 \operatorname{sech}^{2/m}(B_0 X)$ is a solitary bell-shaped non-periodic wave which moves to the right with velocity $(1+c)$.

It is possible to find periodic solutions within each of the above homoclinic loops. The one-parameter family of periodic solutions may be written as

$$\begin{aligned} q_+^k(X) &= \left((A_1 + A\,\mathrm{dn}^2(BX))^{1/m}, -\frac{2}{m} ABk^2 (A_1 + A\,\mathrm{dn}^2(BX))^{1/m-1} \mathrm{dn}(BX)\mathrm{sn}(BX)\mathrm{cn}(BX)\right) \\ q_-^k(X) &= -q_+^k(X) \end{aligned} \tag{10}$$

In Equation (10), dn, sn and cn are the Jacobi elliptic functions and k is the elliptic modulus. The limit $k \to 1$ gives the homoclinic orbit (9). That is, the periodic-wave solution reduces to the solitary-wave solution.

For $m = 1$, the parameters A_1, A and B in Equation (10) are given by

$$A_1 = c\left[1 - \frac{2-k^2}{\sqrt{k^4 - k^2 + 1}}\right], \quad A = \frac{3c}{\sqrt{k^4 - k^2 + 1}}, \quad B = \frac{1}{2\sqrt{\mu}}\sqrt{\frac{c}{1+c}}\,\frac{1}{(k^4 - k^2 + 1)^{1/4}}$$

and for $m = 2$, they are given by

$$A_1 = 0, \quad A = \frac{6c}{2-k^2} \quad \text{and} \quad B = \frac{1}{\mu}\sqrt{\frac{c}{1+c}}\,\frac{1}{\sqrt{2-k^2}}$$

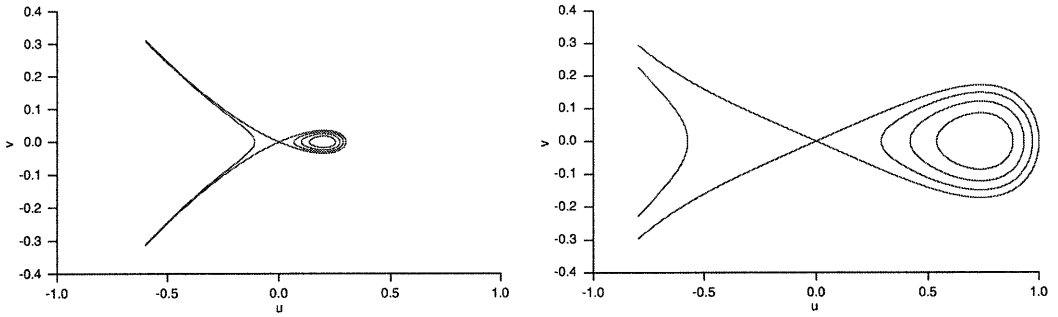

Figure 1. Phase portraits of system (7): Homoclinic orbit and periodic orbits for $m=1$ and 3, respectively.

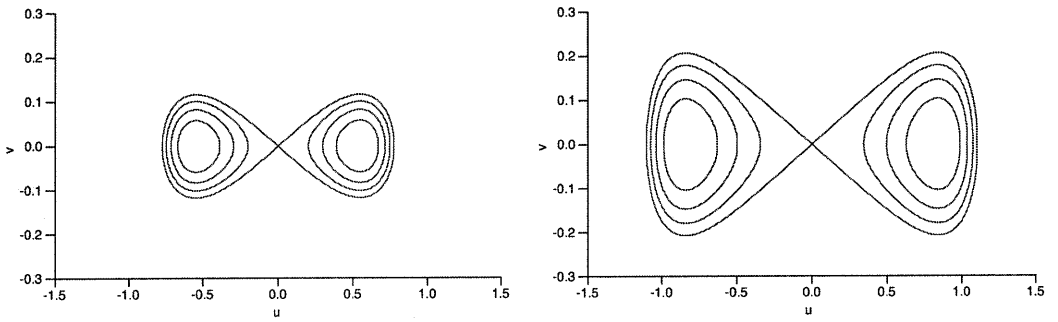

Figure 2. Phase portraits of system (7): Homoclinic and periodic orbits for $m=2$ and 4, respectively.

For $m \neq 1$ or 2, A_1, A and B are determined by the following equations:

$$A_1 = \frac{2c(m+1)(m+2)}{(m^2+4)}, \quad A = \pm A_1 \sqrt{\frac{2-m}{2(1-k^2)}}, \quad B^2 = \frac{m^2 A}{2\mu(1+c)(m+1)(m+2)}$$

and

$$k = \left[\frac{\sqrt{9m^2-28m+36}\ \left(|3m-10| - \sqrt{9m^2-28m+36}\right)}{16(2-m)} \right]^{1/2}$$

From the second equality, it may be seen that the value of A is real only if $m<2$ and $0 \leqslant k<1$. For $m>2$ and $0 \leqslant k<1$, the constant A is complex. However, in Figures 1 and 2, real periodic solutions are plotted for $m>2$. What is happening is that elliptic functions with modulus greater than unity can be related back to elliptic functions with modulus less than unity (see Reference [33]). So, for $m>2$, $k>1$ it follows that A is real. Using elliptic function relations $[\mathrm{sn}(u,k) = k^{-1/2}\,\mathrm{sn}(w,k^{-1})$, $\mathrm{cn}(u,k) = \mathrm{dn}(w,k^{-1})$ and $\mathrm{dn}(u,k) = \mathrm{cn}(w,k^{-1})$, where $w = k^{1/2}u$ and $k>0$; here if $k>1$ then $k^{-1}<1]$, the solution can be related back to elliptic functions with modulus less than unity.

The value of the Hamiltonian function for each periodic orbit is defined as h_k. The period of these orbits is given by

$$T_k = 2K(k)/B \tag{11}$$

where $K(k)$ is a complete elliptic integral of the first kind.

Examples of homoclinic and periodic orbits for $m = 1, 2, 3$ and 4 are shown in Figures 1 and 2, respectively. The values of c and μ are taken to be 0.1 and 1, respectively.

3. LINEARIZED IMPLICIT PSEUDO-SPECTRAL METHOD

Since the RLW equation (3) can be obtained from the generalized RLW (GRLW) equation (4) by just letting $m = 1$ in Equation (4), the linearized pseudo-spectral method is then developed for the GRLW equation (4).

The pseudo-spectral method is a Fourier method in which $u(x,t)$ is transformed into a Fourier space with respect to x, and derivatives (or other operators) with respect to x are then made algebraic in the transformed variable.

For convenience, if the spatial period is normalized to $[0, 2\pi]$, Equation (4) takes the form

$$(u - \mu s^2 u_{XX})_t + s u_X + s u^m u_X = 0 \tag{12}$$

where $X = 2\pi(x-a)/(b-a)$ and $s = 2\pi/(b-a)$. The interval $[0, 2\pi]$ is then discretized by N equidistant points, with spacing $\Delta X = 2\pi/N$. The function $u(X,t)$, numerically defined only on these points, can be transformed to the discrete Fourier space by

$$\hat{u}(\kappa, t) = Fu = \frac{1}{\sqrt{N}} \sum_{j=0}^{N-1} u(j\Delta X, t) e^{-2\pi i j\kappa/N}, \quad \kappa = -\frac{N}{2}, \ldots, -1, 0, 1, \ldots, \frac{N}{2} - 1 \tag{13}$$

The inversion formula is

$$u(j\Delta X, t) = F^{-1}\hat{u} = \frac{1}{\sqrt{N}} \sum_{\kappa=-N/2}^{N/2-1} \hat{u}(\kappa, t) e^{2\pi i j\kappa/N}, \quad j = 0, 1, \ldots, N-1 \tag{14}$$

The implicit pseudo-spectral method for solving Equation (12) is given by

$$\begin{aligned} &u(X, t+\Delta t) - u(X,t) - \mu s^2 u(X, t+\Delta t) + \mu s^2 u(X,t) \\ &\quad = -\frac{1}{2(m+1)} s\Delta t(\{u(X,t)\}^{m+1} + \{u(X, t+\Delta t)\}^{m+1})_X \\ &\quad\quad -\frac{1}{2} s\Delta t(u_X(X,t) + u_X(X, t+\Delta t)) \end{aligned} \tag{15}$$

To find $u(X, t+\Delta t)$ from $u(X,t)$, a set of non-linear algebraic equations has to be solved. To overcome this difficulty, a way of linearizing the implicit pseudo-spectral method (15) is presented.

The linearized form is obtained simply by expanding $\{u(X,t+\Delta t)\}^{m+1}$ using Taylor's series. That is,

$$\{u(X,t+\Delta t)\}^{m+1} = \{u(X,t)\}^{m+1} + A_T \Delta u + O(\Delta t^2) \tag{16}$$

where $A_T = \mathrm{d}u^{m+1}(X,t)/\mathrm{d}u = (m+1)\{u(X,t)\}^m$ and $\Delta u = u(X,t+\Delta t) - u(X,t)$

Substituting Equation (16) into Equation (15), leads to

$$\begin{aligned} &u(X,t+\Delta t) - u(X,t) - \mu s^2[u_{XX}(X,t+\Delta t) - u_{XX}(X,t)] \\ &\quad = -\frac{s}{2}\Delta t(u_X(X,t) + u_X(X,t+\Delta t)) - \frac{s}{2(m+1)}\Delta t((1-m)\{u(X,t)\}^{m+1} \\ &\quad + (1+m)u(X,t+\Delta t)\{u(X,t)\}^m)_X \end{aligned} \tag{17}$$

which after rearranging can be written as

$$\begin{aligned} &u(X,t+\Delta t) + \frac{s}{2}\Delta t(u(X,t+\Delta t)\{u(X,t)\}^m)_X + \frac{s}{2}\Delta t\, u_X(X,t+\Delta t) - \mu s^2 u_{XX}(X,t+\Delta t) \\ &\quad = u(X,t) - \frac{(1-m)s}{2(1+m)}\Delta t(\{u(X,t)\}^{m+1})_X - \frac{s}{2}\Delta t\, u(X,t) - \mu s^2 u_{XX}(X,t) \end{aligned} \tag{18}$$

or

$$\begin{aligned} &u(X,t+\Delta t) + \frac{s}{2}\Delta t(\{u(X,t)\}^m u_X(X,t+\Delta t) + m\{u(X,t)\}^{m-1}u_X(X,t)u(X,t+\Delta t)) \\ &\quad + \frac{s}{2}\Delta t\, u(X,t+\Delta t) - \mu s^2 u_{XX}(X,t+\Delta t) \\ &\quad = u(X,t) - \frac{s}{2}\Delta t\, u(X,t) - \frac{(1-m)s}{2}\Delta t(\{u(X,t)\}^m u_X(X,t)) - \mu s^2 u_{XX}(X,t+\Delta t) \end{aligned} \tag{19}$$

Using Equation (14), Equation (19) (with $X = j\Delta X$) becomes

$$\begin{aligned} &\frac{1}{\sqrt{N}}\sum_{\kappa=-N/2}^{N/2-1}\left[1 + \frac{ms}{2}\Delta t\{u(j\Delta X,t)\}^{m-1}u_X(j\Delta X,t) + \frac{s}{2}\Delta t(1 + \{u(j\Delta X,t)\}^m)\mathrm{i}\kappa + \mu s^2\kappa^2\right] \\ &\quad \times \hat{u}(\kappa,t+\Delta t)\mathrm{e}^{2\pi \mathrm{i} j\kappa/N} = S_3(j\Delta X,t), \quad j = 0,1,\ldots,N-1 \end{aligned} \tag{20}$$

where $S_3(j\Delta X,t)$, $j=0,1,\ldots,N-1$ is the right-hand side of Equation (19), which can be calculated (using the fast Fourier transform [34] for $u_X(X,t) = F^{-1}\{\mathrm{i}\kappa F u\}$ and $u_{XX}(X,t) = F^{-1}\{-\kappa^2 F u\}$) at each time step.

To find $\hat{u}(\kappa,t+\Delta t)$, $\kappa = -N/2,\ldots,-1,0,1,\ldots,N/2-1$, the linear system of order N given by Equation (20) needs to be solved at each time step. This approach is time consuming.

A way to avoid this problem is to use a one-point iteration scheme in the form

$$\frac{1}{\sqrt{N}}\sum_{\kappa=-N/2}^{N/2-1}\left(1+\mu s^2\kappa^2+\frac{1}{2}s\Delta t\,\mathrm{i}\kappa\right)\hat{u}^{(n)}(\kappa,t+\Delta t)\mathrm{e}^{2\pi\mathrm{i}j\kappa/N}$$

$$=S_3(j\Delta X,t)-\frac{ms}{2}\Delta t\{u(j\Delta X,t)\}^{m-1}u_X(j\Delta X,t)\left\{\frac{1}{\sqrt{N}}\sum_{\kappa=-N/2}^{N/2-1}\hat{u}^{(n-1)}(\kappa,t+\Delta t)\mathrm{e}^{2\pi\mathrm{i}j\kappa/N}\right\}$$

$$-\frac{s}{2}\Delta t\{u(j\Delta X,t)\}^m\left\{\frac{1}{\sqrt{N}}\sum_{\kappa=-N/2}^{N/2-1}\mathrm{i}\kappa\,\hat{u}^{(n-1)}(\kappa,t+\Delta t)\mathrm{e}^{2\pi\mathrm{i}j\kappa/N}\right\},\quad n=1,2,\ldots \tag{21}$$

with an initial approximation $\hat{u}^{(0)}$ at each time step taken to be $\hat{u}^{(0)}(\kappa,t+\Delta t)=\hat{u}(\kappa,t)$ (see Equation (13)).

The transforms in Equation (21) are performed using the fast Fourier transform algorithm. Once $\hat{u}^{(n)}(\kappa,t+\Delta t)$, $\kappa=-N/2,\ldots,-1,0,1,\ldots,N/2-1$ is found, it can be used to calculate $u(j\Delta x,t+\Delta t)$, $j=0,1,\ldots,N-1$ from Equation (14). Computationally, this approach is found to be economical, since only a very few iterations are needed at each time step for the method to attain convergence. The criterion used for stopping the iterations at each time step is

$$\left\|\frac{1}{\sqrt{N}}\sum_{\kappa=-N/2}^{N/2-1}\hat{u}^{(n)}(\kappa,t+\Delta t)\mathrm{e}^{2\pi\mathrm{i}j\kappa/N}-\frac{1}{\sqrt{N}}\sum_{\kappa=-N/2}^{N/2-1}\hat{u}^{(n-1)}(\kappa,t+\Delta t)\mathrm{e}^{2\pi\mathrm{i}j\kappa/N}\right\|_\infty<\varepsilon$$

for some n and some tolerance $\varepsilon>0$.

Remark

The solutions to the original RLW equation can be obtained from Equation (21) (with $m=1$).

In the same way as in the GRLW equation, the linearized implicit pseudo-spectral method can be extended to the general non-linear wave Equations (2).

Again, for convenience, the spatial period is normalized to $[0,2\pi]$, then Equation (2) can be transformed into

$$u_t+su_X+s[F(u)]_X+c(Hu)_t=0 \tag{22}$$

where $F'(u)=\mathrm{d}F(u)/\mathrm{d}u=f(u)$ and c is a constant which is related to the linear operator H (for example, for the case of the RLW equation where $H=-\partial^2/\partial x^2$, $c=s^2$).

The linearized implicit pseudo-spectral method for solving Equation (22) is given by

$$u(X,t+\Delta t)+\frac{s}{2}\Delta t(f\{u(X,t)\}u_X(X,t+\Delta t)$$

$$+f'\{u(X,t)\}u_X(X,t)u(X,t+\Delta t))+cHu(X,t+\Delta t)$$

$$=u(X,t)-\frac{s}{2}\Delta t(f\{u(X,t)\}-u(X,t)f'\{u(X,t)\})u_X(X,t)+cHu(X,t) \tag{23}$$

4. LINEAR STABILITY ANALYSIS OF THE NUMERICAL METHOD

In an attempt to gain some insight into the stability of method (19), linear stability analysis is used to analyse the method. This entails first of all, locally freezing one variable in the non-linear convective term, namely, $u^m u_x = v u_x$, where v is a locally constant value of u^m, then employing the standard Fourier analysis to determine the condition which has to be imposed on the time step Δt for stability. Although the application of the linear stability analysis to non-linear equations cannot be rigorously justified, it provides, however, the necessary conditions for stability, and it is found to be effective in practice (see, for example, References [10, 12, 24, 25]).

In the following, it will be shown that the linearized implicit pseudo-spectral method for the generalized RLW equation is unconditionally stable.

Consider the locally constant equation

$$u_t + u_x + v u_x - \mu u_{xxt} = 0, \quad v \text{ constant} \tag{24}$$

approximated using the proposed method by

$$\begin{aligned} u(x,t+\Delta t) - u(x,t) = &-\tfrac{1}{2}(1+v)\Delta t(F^{-1}\{\mathrm{i}\kappa F u(x,t+\Delta t)\} + F^{-1}\{\mathrm{i}\kappa F u(x,t)\}) \\ &- \mu(F^{-1}\{-\kappa^2 F u(x,t+\Delta t)\} - F^{-1}\{-\kappa^2 F u(x,t)\}) \end{aligned} \tag{25}$$

Using the standard Fourier analysis, a solution to (25) of the form

$$u(x,t) = \zeta^{t/\Delta t} \mathrm{e}^{\mathrm{i}\kappa x} \tag{26}$$

is sought. Substituting Equation (26) into Equation (25) leads to

$$\begin{aligned} &\zeta^{(t+\Delta t)/\Delta t}\mathrm{e}^{\mathrm{i}\kappa x} + \tfrac{1}{2}\,\mathrm{i}\kappa(1+v)\Delta t\,\zeta^{(t+\Delta t)/\Delta t}\mathrm{e}^{\mathrm{i}\kappa x} + \mu\kappa^2\,\zeta^{(t+\Delta t)/\Delta t}\mathrm{e}^{\mathrm{i}\kappa x} \\ &= \zeta^{t/\Delta t}\mathrm{e}^{\mathrm{i}\kappa x} - \tfrac{1}{2}\,\mathrm{i}\kappa(1+v)\Delta t\,\zeta^{t/\Delta t}\mathrm{e}^{\mathrm{i}\kappa x} + \mu\kappa^2\,\zeta^{t/\Delta t}\mathrm{e}^{\mathrm{i}\kappa x} \end{aligned} \tag{27}$$

or

$$\zeta = \frac{1 + \mu\kappa^2 - \frac{1}{2}\,\mathrm{i}\kappa\Delta t(1+v)}{1 + \mu\kappa^2 + \frac{1}{2}\,\mathrm{i}\kappa\Delta t(1+v)} \tag{28}$$

From Equation (28), it can be deduced that the linearized implicit pseudo-spectral method is unconditionally stable since $|\zeta| = 1$.

5. NUMERICAL RESULTS

To illustrate the effectiveness of the linearized implicit pseudo-spectral method, numerical results portraying a single soliton solution and the collision of two solitons are reported for the RLW and the GRLW equations. The numerical results obtained are compared to the analytical solution (whenever the analytical solution is known), each providing corroborative evidence of the findings of the other.

5.1. The RLW and the GRLW equations

Single soliton case: Numerical computations of the original RLW equation have been repeated often in the literature. To show the effectiveness of the proposed linearized implicit pseudo-spectral method, however, two cases corresponding to $m=1$ and 2 are described for the RLW and the GRLW equations.

The analytical solution of (4) on the infinite interval is

$$u(x,t)=\{D\,\mathrm{sech}^2[K(x-(1+c)t-x_0)]\}^{1/m} \tag{29}$$

where

$$D=\frac{(m+1)(m+2)c}{2},\quad K=\frac{m}{2\sqrt{\mu}}\sqrt{\frac{c}{1+c}},\quad x_0=\text{constant}$$

For initial conditions, Equation (29) is used at $t=0$ with some values of c and μ, and x_0 is chosen to be zero. For boundary conditions, periodic boundary conditions on the interval $[a,b]$ are imposed.

Taking $\Delta t=0.1$ and subdividing the x-interval into $N=128$ subintervals $\Delta x=(b-a)/N=0.78125$, problem (4) for $m=1$ and 2 was integrated from $t=0$ to 20 and in the region $-40<x<60$. The results obtained in Tables I–III are found using the one-point iteration scheme (21) with $x_0=0$, $c=0.1$ and tolerance $\varepsilon=0.0001$. The CPU times needed to reach times $t=20$ for $m=1$ and 2 using the linearized implicit pseudo-spectral method (21) were 12.02 and 12.45 s, respectively. The error norms for the solitary wave of the GRLW equation with $m=1$ and 2, are given in Tables I and II, respectively. Throughout the simulation the L_2 and L_∞ error norms remain less than 2×10^{-4} and 7×10^{-5} (for the RLW equation with $m=1$), and 2×10^{-3} and 5×10^{-4} (for the GRLW equation with $m=2$). A comparison with other methods [16, 20, 21, 23], shows that the error norms at time $t=20$ (for the RLW equation with $m=1$), found with the present method, are smaller than those obtained with those four methods (see, Table I). Moreover, it can be seen from Table III that the linearized implicit pseudo-spectral method (for the GRLW equation with $m=1$ and 2) produced noticeable reductions in error when the time step is decreased ($\Delta t=0.05$). Increasing the space and the time steps were also found to produce results that are reasonably accurate and within a few seconds of CPU time.

The profile of the solitary waves for the GRLW equation with $m=1$ and 2, from time $t=0$ to 20, are depicted in Figure 3. From this figure, it can be seen that the solitary wave moves to the right unchanged in form, and as m increases, the speed velocity of the wave decreases and the amplitude increases as time increases (that is, wave increases in height and width).

As the existence of conservation laws [28] has been shown to be a characteristic property of soliton-producing equations, the conserved quantities of the mass $M(t)=\int_a^b u\,\mathrm{d}x$, momentum $P(t)=\int_a^b(u^2+\mu u_x^2)\,\mathrm{d}x$ and energy $E(t)=\int_a^b(u^3+3u^2)\,\mathrm{d}x$ [13] are used to provide checks on the numerical integrations. The invariants $M(t)$, $P(t)$ and $E(t)$ (for the GRLW equation with $m=1$ and 2) at different values of time t are recorded in Tables I–III. From these tables, it can be seen that the conservation properties (using the linearized pseudo-spectral method) are very good. In comparison with the analytical values for the invariants given by $M_{\mathrm{ex}}=6c/K=3.9799497$, $P_{\mathrm{ex}}=(12c^2/K)+(48Kc^2\mu/5)=0.81046249$ and $E_{\mathrm{ex}}=(36c^2/K)+(144c^3/5K)=2.579007$ [23], for $m=1$ and $c=0.1$, the relative changes in the invariants are very small (the quantities M, P and E change by less than 8×10^{-4}per cent, 6×10^{-5}per cent

Table I. Single solitary wave for the RLW equation ($m=1$); $c=0.1$ (amplitude 0.3), $\Delta t=0.1$, $-40\leqslant x\leqslant 60$.

Method	Time	L_∞	L_2	M	P	E
Pseudo-spectral	0	0.000	0.000	3.97993	0.810462	2.57901
	4	0.134×10^{-4}	0.381×10^{-4}	3.97993	0.810462	2.57901
	8	0.269×10^{-4}	0.749×10^{-4}	3.97993	0.810462	2.57901
	12	0.408×10^{-4}	0.111×10^{-3}	3.97993	0.810462	2.57901
	16	0.536×10^{-4}	0.147×10^{-3}	3.97993	0.810462	2.57901
	20	0.666×10^{-4}	0.182×10^{-3}	3.97992	0.810462	2.57901
Petrov Galerkin quadratic [23]	20	0.810×10^{-4}	0.227×10^{-3}	3.97986	0.810399	2.57880
Least-square linear [21]	20	17.55×10^{-4}	4.688×10^{-3}	3.98203	0.808650	2.57302
Galerkin quadratic [20]	20	0.860×10^{-4}	0.220×10^{-3}	3.97989	0.810467	2.57902
Finite-difference cubic [16]	20	673.5×10^{-4}	196.1×10^{-3}	4.41219	0.897342	2.85361

Table II. Single solitary wave for the RLW equation ($m=2$) using Equation (21); $c=0.1$, $\Delta t=0.1$, $-40\leqslant x\leqslant 60$.

Time	L_∞	L_2	M	P	E
0	0.000	0.000	8.07087	4.10055	14.36112
4	0.112×10^{-3}	0.266×10^{-3}	8.07088	4.10055	14.36111
8	0.226×10^{-3}	0.524×10^{-3}	8.07087	4.10055	14.36110
12	0.326×10^{-3}	0.771×10^{-3}	8.07087	4.10055	14.36110
16	0.410×10^{-3}	0.101×10^{-2}	8.07087	4.10055	14.36107
20	0.496×10^{-3}	0.123×10^{-2}	8.07086	4.10054	14.36106

Table III. Single solitary wave for the RLW equation (with $m=1$ and 2) using Equation (21); $c=0.1$, $\Delta t=0.05$, $-40\leqslant x\leqslant 60$.

m	Time	L_∞	L_2	M	P	E
1	4	0.511×10^{-5}	0.118×10^{-4}	3.97993	0.810462	2.57901
	12	0.102×10^{-4}	0.289×10^{-4}	3.97993	0.810462	2.57901
	20	0.167×10^{-4}	0.491×10^{-4}	3.97992	0.810462	2.57901
2	4	0.208×10^{-4}	0.505×10^{-4}	8.07088	4.10055	14.36112
	12	0.570×10^{-4}	0.146×10^{-3}	8.07087	4.10055	14.36111
	20	0.910×10^{-4}	0.237×10^{-3}	8.07088	4.10055	14.36111

and 2×10^{-4}per cent, respectively, by $t=20$). This degree of conservation is superior to that found with other methods listed (see, Table I).

In the second experiment, a smaller solitary wave of amplitude 0.09 ($c=0.03$) has been modelled, and the results of simulation are given in Table IV (for $m=1$). As the amplitude of the solitary wave is reduced the pulse broadens and it may be necessary to increase the

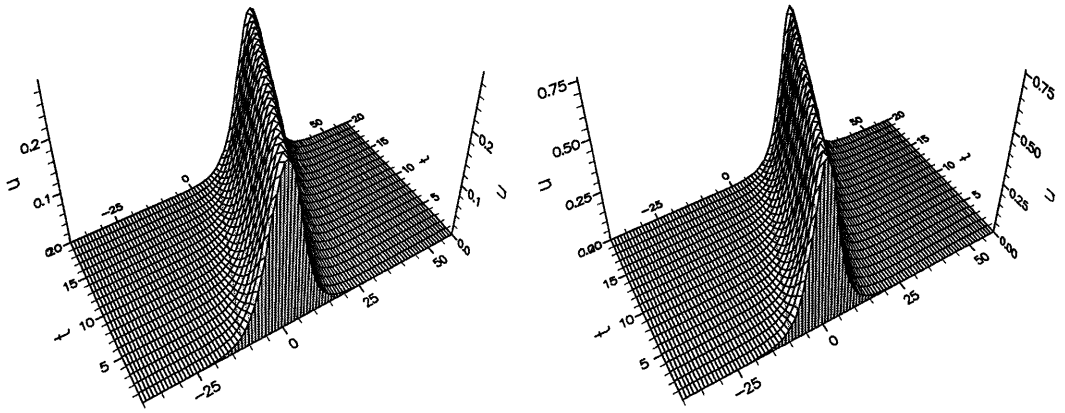

Figure 3. Single solitary wave for the GRLW equation with $m=1$ and 2, respectively; $c=0.1$.

Table IV. Single solitary wave for the RLW equation ($m=1$); $c=0.03$ (amplitude 0.09), $\Delta t=0.1$, $-80\leqslant x\leqslant 120$.

Method	Time	L_∞	L_2	M	P	E
Pseudo-spectral	0	0.000	0.000	2.109405	0.127302	0.388806
	4	0.760×10^{-6}	0.275×10^{-5}	2.109406	0.127302	0.388806
	8	0.155×10^{-5}	0.543×10^{-5}	2.109405	0.127302	0.388806
	12	0.231×10^{-5}	0.810×10^{-5}	2.109405	0.127302	0.388806
	16	0.316×10^{-5}	0.108×10^{-4}	2.109406	0.127302	0.388806
	20	0.392×10^{-5}	0.134×10^{-4}	2.109405	0.127302	0.388806
Petrov Galerkin quadratic [23]	20	0.230×10^{-4}	0.530×10^{-4}	—	—	—

solution range in order to maintain accuracy. The range here is doubled from $-40\leqslant x\leqslant 60$ to $-80\leqslant x\leqslant 120$.

The error norms and the invariants for $c=0.03$, are recorded in Tables IV–VI for different values of time t. With the range $-80\leqslant x\leqslant 120$, $\Delta t=0.1$, excellent results were obtained (Tables IV, V). Throughout the simulation the L_2 and L_∞ error norms remain less than 2×10^{-5} and 4×10^{-6} for the RLW equation with $m=1$, and 2×10^{-4} and 5×10^{-5} for the GRLW equation with $m=2$. Moreover, it can be seen that the error norms (L_2 and L_∞) are small compared with those quoted by other authors [23]. Decreasing the time step from 0.1 to 0.05, is found to produce noticeable reduction in errors for the error norms (see Table VI).

The invariants $M(t)$, $P(t)$ and $E(t)$ (for the GRLW equation with $m=1$ and 2) at different values of time t are also recorded in Tables IV–VI, where it can be seen that (using the linearized pseudo-spectral method) the invariants remain constant with respect to time t. In comparison with the analytical values ($M_{ex}=2.109407$, $P_{ex}=0.127302$ and $E_{ex}=0.388806$) for $m=1$, it can be seen from Table IV that the quantities M, P and E obtained (using the linearized pseudo-spectral method (21)) are very close to the corresponding analytical values.

Table V. Single solitary wave for the RLW equation ($m=2$) using Equation (21); $c=0.03$, $\Delta t=0.1$, $-80\leqslant x\leqslant 120$.

Time	L_∞	L_2	M	P	E
0	0.000	0.000	7.80987	2.12989	7.03111
4	0.948×10^{-5}	0.280×10^{-4}	7.80987	2.12989	7.03111
8	0.196×10^{-4}	0.559×10^{-4}	7.80987	2.12989	7.03111
12	0.288×10^{-4}	0.835×10^{-4}	7.80987	2.12989	7.03111
16	0.394×10^{-4}	0.111×10^{-3}	7.80987	2.12989	7.03111
20	0.474×10^{-4}	0.137×10^{-3}	7.80987	2.12989	7.03111

Table VI. Single solitary wave for the RLW equation using Equation (21); $c=0.03$, $\Delta t=0.05$, $-80\leqslant x\leqslant 120$.

m	Time	L_∞	L_2	M	P	E
1	4	0.355×10^{-6}	0.853×10^{-6}	2.10941	0.12730	0.38881
	12	0.579×10^{-6}	0.211×10^{-5}	2.10941	0.12730	0.38881
	20	0.930×10^{-6}	0.342×10^{-5}	2.10941	0.12730	0.38881
2	4	0.237×10^{-5}	0.711×10^{-5}	7.80987	2.12989	7.03111
	12	0.721×10^{-5}	0.209×10^{-5}	7.80987	2.12989	7.03111
	20	0.118×10^{-4}	0.344×10^{-4}	7.80987	2.12989	7.03111

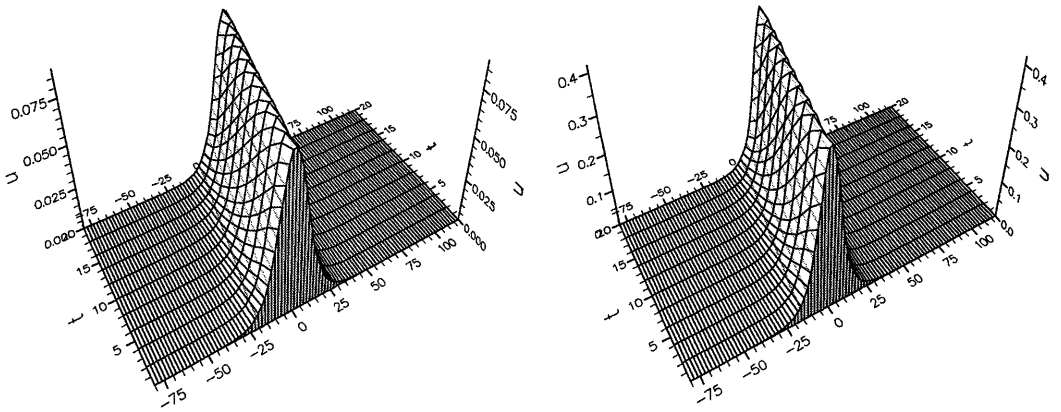

Figure 4. Single solitary wave for the GRLW equation with $m=1$ and 2, respectively; $c=0.03$.

The numerical results for the GRLW equation with $m=1$ and 2 are shown in Figure 4 (for a single soliton with $c=0.03$), in which it can be seen that the solitary wave propagates in a stable fashion (and unchanged in form).

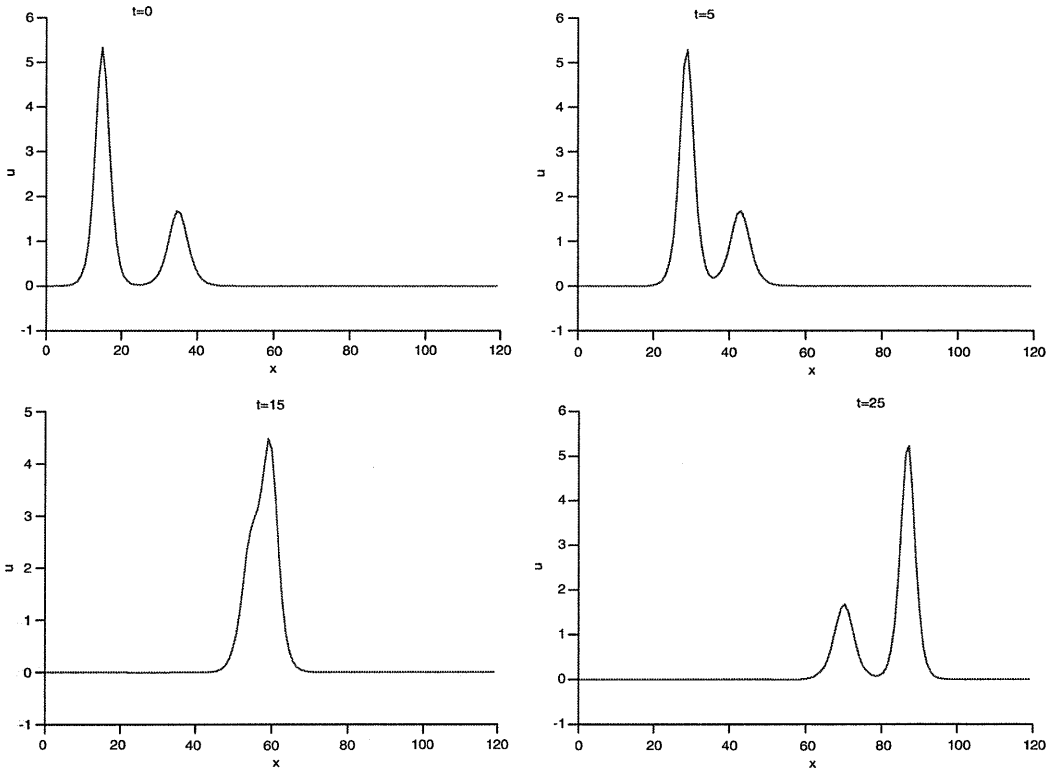

Figure 5. Solitary wave interaction for the RLW equation with $m=1$ at $t=0$, 5, 15 and 25.

Soliton interaction: Here the interaction of two solitons is studied. The initial condition is given by

$$u(x,0)=\sum_{i=1}^{2} D_i \operatorname{sech}^2[K_i(x-(1+c_i)t-x_i)]^{1/m} \tag{30}$$

where

$$D_i=\frac{(m+1)(m+2)c_i}{2}, \quad K_i=\frac{m}{2\sqrt{\mu}}\sqrt{\frac{c_i}{1+c_i}}$$

To allow the interaction to take place, the experiment was run from $t=0$ to 25 and in the region $0<x<120$ for the case $m=1$, and from $t=0$ to 200, $0<x<300$ for $m=2$. Figures 5, 6 show the interaction of two soliton solutions of the GRLW equation (with $m=1$ and 2) for $\mu=1$, $K_1=0.4$, $K_2=0.3$, $x_1=15$, $x_2=35$, $\Delta t=0.1$ and $N=128$. From these figures, it can be seen that the faster pulse interacts with, and emerges ahead of, the slower pulse, with the shape and velocity of each soliton retained. Under magnification of Figure 5 ($t=25$, $m=1$), an oscillation of small amplitude, average $\approx 2\times 10^{-3}$, trailing behind the solitary waves, was observed. This is in accordance with the observations of Abdulloev *et al.* [9], Gardner *et al.* [11] and Soliman *et al.* [12]. The solitary wave interaction in Figure 6 for $m=2$ shows

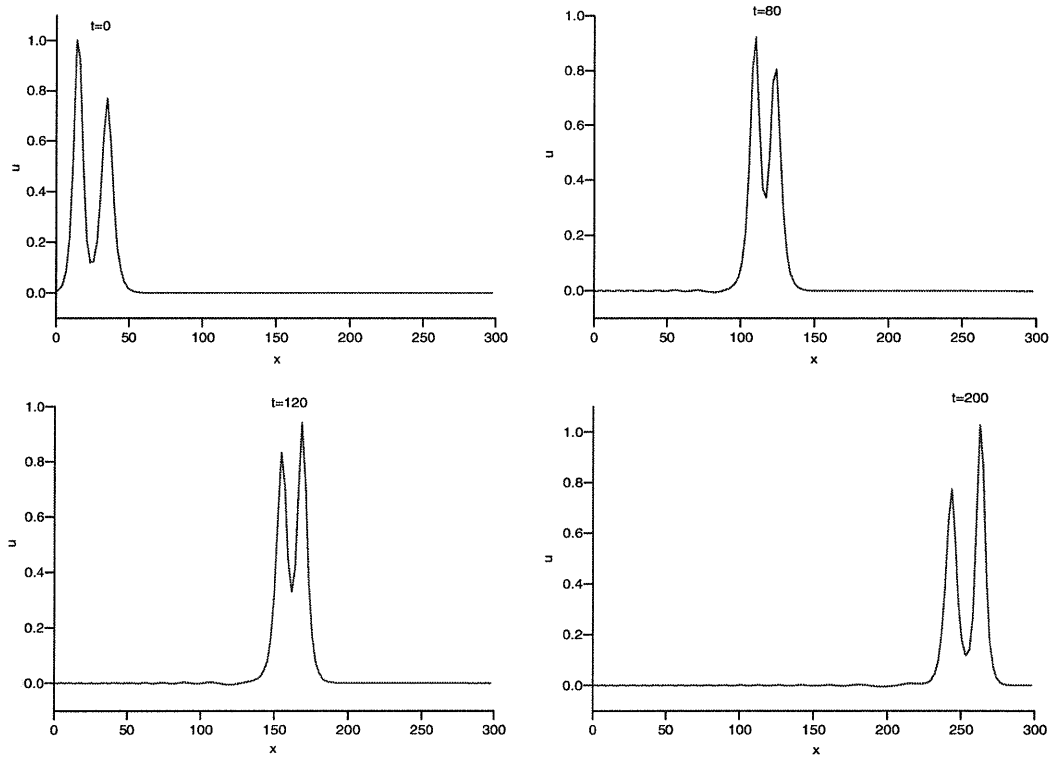

Figure 6. Solitary wave interaction for the GRLW equation with $m=2$ at $t=0$, 80, 120 and 200.

Table VII. Invariants for solitary wave interaction; $m=1$, $\Delta t=0.1$, $0\leqslant x\leqslant 120$.

$m=1$	M	P	E
$t=0$	37.917	120.523	744.081
$t=5$	37.917	120.525	744.088
$t=10$	37.917	120.471	743.518
$t=15$	37.917	120.326	741.974
$t=20$	37.916	120.519	744.021
$t=25$	37.917	120.537	744.191

clearly some evidence of an additional disturbance. Under magnification, an oscillation of amplitude $\approx 2\times 10^{-2}$ is trailing behind the solitary waves. This may be due to the fact that the regularized RLW equation, and its generalized form, are not completely integrable.

As before, a numerical check on the conservation of mass, momentum and energy shows that the three quantities remain constant with respect to time t (see, Tables VII and IX for $m=1$ and 2, respectively). By decreasing the time step (Table VIII), it can be seen that the degree of conservation is much better, and is far better to that found with other methods [12].

Table VIII. Invariants for solitary wave interaction; $m=1$, $\Delta t=0.01$, $0\leqslant x\leqslant 120$.

$m=1$	M	P	E	M[12]	P[12]	E[12]
$t=0$	37.917	120.523	744.081	37.916	120.519	744.082
$t=5$	37.917	120.523	744.078	38.009	120.622	744.755
$t=10$	37.917	120.522	744.068	38.089	121.883	746.771
$t=15$	37.917	120.520	744.052	38.149	121.075	748.243
$t=20$	37.917	120.522	744.070	38.248	121.274	749.834
$t=25$	37.917	120.522	744.068	38.362	121.464	751.303

Table IX. Invariants for solitary wave interaction; $m=2$, $\Delta t=0.1$, $0\leqslant x\leqslant 300$.

$m=2$	M	P	E
$t=0$	16.448	10.218	36.702
$t=40$	16.455	10.222	36.731
$t=80$	16.454	10.223	36.772
$t=120$	16.455	10.226	36.790
$t=160$	16.456	10.230	36.772
$t=200$	16.457	10.222	36.730

6. SUMMARY AND CONCLUSIONS

A linearized implicit pseudo-spectral method is developed for the RLW equation, and its generalized form. The method proposed was tested on problems from the literature. Numerical experiments for the RLW equation, and its generalized form ($m=1$ and 2) were reported for a single soliton and the interaction of two solitons.

An important advantage to be gained from the use of this method is the ability to produce very accurate results on a reasonably coarse mesh. Using the linearized stability analysis, it is shown that the proposed method is unconditionally stable.

The method described here is for the RLW equation, and its generalized form, but it can be implemented to a broad class of non-linear wave equations of form (2), with obvious changes in the various formulae.

REFERENCES

1. Russell JS. Report on waves. *Report on 14th Meeting of the British Association for the Advancement of Science*. John Murray: London, 1844; 311–390.
2. Stokes GG. On the theory of oscillatory waves. *Cambridge Transactions* 1847; **8**:441–472.
3. Boussinesq J. Theorie des ondes et des remous qui se propagent le long d'un canal rectangulaire horizontal, en communiquant au liquide contenu dans ce canal des vitesses sensiblement parailles de la surface au fond. *Journal de Mathematiques Pures et Appliques* 1872; **17**:55–108.
4. Rayleigh B. On waves. *Philosophical Magazine* 1876; **5**(1):257–279.
5. Korteweg DJ, de Vries G. On the change of form of long waves advancing in a rectangular channel, and a new type of long stationary wave. *Philosophical Magazine Series 5* 1895; **39**:422–443.
6. Peregrine DH. Calculations of the development of an undular bore. *Journal of Fluid Mechanics* 1966; **25**: 321–330.
7. Benjamin TB, Bona JL, Mahoney JJ. Model equations for long waves in nonlinear dispersive waves. *Journal of Computational Physics* 1972; **30**:428–451.

8. Craig W, Groves M. Hamiltonian long-wave approximations to the water-wave problem. *Wave Motion* 1994; **19**:367–389.
9. Abdulloev KhO, Bogalubsky H, Markhankov VG, On more example of inelastic soliton interaction. *Physics Letters* 1976; **56A**:427–428.
10. Sloan DM, Fourier pseudospectral solution of the regularized long wave equation. *Journal of Computational and Applied Mathematics* 1991; **36**:159–179.
11. Gardner LRT, Gardner GA. Solitary waves of the regularized long-wave equation. *Journal of Computational Physics* 1990; **91**:441–459.
12. Soliman AA, Raslan KR. Collocation method using quadratic B-spline for the RLW equation. *International Journal of Computer Mathematics* 2001; **78**:399–412.
13. Olver PJ. Euler operators and conservation laws of the BBM equation. *Mathematical Proceedings of the Cambridge Philosophical Society* 1979; **85**:143–159.
14. Eilbeck JC, MaGuire GR. Numerical study of RLW equation I: numerical methods. *Journal of Computational Physics* 1975; **19**:43–62.
15. Jain PC, Iskandar L. Numerical solution of the RLW equation. *Computer Methods in Applied Mechanics and Engineering* 1985; **20**:195–200.
16. Jain PC, Shankar R, Singh TV. Numerical solution of regularized long-wave equation. *Communications in Numerical Methods and Engineering* 1993; **9**:579–586.
17. Bahrdwaj D, Shankar R. A computational method for regularized long wave equation. *Computational Mathematics and Applications* 2000; **40**:1397–1404.
18. Wahlbin L. *Numerische Mathematik* 1975; **23**:289–303.
19. Alexander ME, Morris JLl. Galerkin method applied to some model equations for nonlinear dispersive waves. *Journal of Computational Physics* 1979; **30**:428–451.
20. Gardner LRT, Gardner GA, Dag I. A B-spline finite element method for the regularized long wave equation. *Communications in Numerical Methods and Engineering* 1995; **11**:59–68.
21. Gardner LRT, Gardner GA, Dogan A. A least-squares finite element scheme for the RLW equation. *Communications in Numerical Methods and Engineering* 1996; **12**:795–804.
22. Dag I, Ozer MN. Approximation of the RLW equation by the least square cubic B-spline finite element method. *Applied Mathematical Modelling* 2001; **25**:221–231.
23. Dogan A. Numerical solution of regularized long wave equation using Petrov–Galerkin method. *Communications in Numerical Methods and Engineering* 2001; **17**:485–494.
24. Djidjeli K, Price WG, Temarel P, Twizell EH. A linearized implicit pseudo-spectral method for certain non-linear wave equations. *Communications in Numerical Methods and Engineering* 1998; **14**:977–993.
25. Fornberg B, Whitham GB. A numerical and theoretical study of certain nonlinear wave phenomena. *Philosophical Transactions of the Royal Society of London* 1978; **A289**:373–404.
26. Bona JL, McKinney WR, Restrepo JM. Stable and unstable solitary-wave solutions of the generalized regularized long-wave equation. *Journal of Nonlinear Science* 2000; **10**:603–638.
27. Whitham GB. *Linear and Nonlinear Waves.* Wiley: New York, 1974.
28. Drazin PG, Johnson RS. *Solitons: An Introduction.* Cambridge University Press: Cambridge, MA, 1989.
29. Thompson JMT. Chaotic phenomena triggering the escape from a potential well. *Proceedings of the Royal Society of London* 1989; **A421**:195–225.
30. Rubio MA, De La Torre M, Antoranz JC. Intermittencies and power-law low frequency divergencies in a nonlinear oscillator. *Physica D* 1989; **36**:92–108.
31. Senjanovic I, Fan Y. Dynamic analysis of ship capsizing in regular waves. *Brodogradnja* 1994; **42**:51–60.
32. Guckenheimer J, Holmes P. *Nonlinear Oscillations, Dynamical Systems, and Bifurcations of Vector Fields.* Springer: Berlin, 1983.
33. Abramowitz M, Stegun IA, *Handbook of Mathematical Functions.* Dover: New York, 1965.
34. Cooley JW, Lewis PAW, Welch PD. The fast Fourier transform and its applications. *IEEE Transactions on Education E12* 1969; **1**:27–34.

